Simplified Equivalent Representations for Multicoupled Lines and their Application to Filter Design

HIROAKI KUNIEDA

Abstract—This paper presents simplified lumped-type equivalent representations, which are equivalent to multiwire lines in the vicinity of a quarter-wavelength frequency. It is believed that the derived representations can easily be applied to the analysis and the design of coupled-line filters and directional couplers of narrow bandwidths composed of quarter-wavelength strips.

In this paper, the general design method for coupled-line bandpass filters is presented as one of the applications. A new bandpass filter is proposed and the design formulas of the filter are derived by using the design method. Furthermore, the range of validity of the derived representations has been checked by showing numerical design examples. They have been found to give excellent results for coupled-line filters of bandwidths up to about 30 percent.

I. Introduction

GRAPH REPRESENTATION is widely known as the equivalent circuit of the multiwire-line network [1]. It consists of distributed inductances and uncoupled unit elements in terms of Richards' variable ($p=\tanh(\gamma l)$). This graph transformation method is often useful in yielding the equivalent circuits of coupled-line filters and other circuit elements.

Since this graph representation consists of two-port elements as unit elements, it sometimes requires special techniques for circuit transformations and also it is not easy to apply computer aided design methods.

To avoid these disadvantages, lumped-element equivalent representations by use of a half-angle Richards' variable ($\tilde{q}=2\tanh(\gamma l/2)$) were proposed by M. Onoda and the author [2]. The derived representations were useful for analysis but not easily applied to design filters.

On the other hand, coupled-line filters and directional couplers of narrow bandwidths are particularly useful in practical microwave systems. Therefore, useable simplified lumped-element equivalent representations for multiwire lines are required for both analysis and synthesis even if they are only approximately valid in the vicinity of the quarter-wavelength frequency f_0.

This paper presents simplified lumped-element equivalent representations for multiwire lines by introducing a new variable ($q=2\tanh(j(\pi/4)((f/f_0)-1))$). The derived representations are useful under about 5-percent relative error in the frequency range $0.85<f/f_0<1.15$. The representations consist of an ideal immittance–inverter bank and distributed capacitances or inductances in terms of this q-variable.

Both exact [3] and approximate design methods [4]–[9] of distributed coupled-line filters have been reported previously. As an application of the new representation, a new approximate design method of coupled-line filters is proposed. The design method can uniformly be applied to various types of coupled-line filters. Several new and improved results are obtained. In particular, this paper shows that the new design method leads to the equivalent circuits of coupled-line filters easily and does not require any special techniques. And it shows that the model expressed by the inductance matrix with inductive couplings between nearest and next-nearest neighbors is adequate and preferable over a sparse capacitance-matrix design for coupled-line filters with comparatively many open-circuited terminals. Furthermore, this paper proposes a new type of bandpass filter. Design examples of new bandpass filters and hairpin-line filters show that the sparse capacitance matrices designed by the proposed method give exact responses for relative bandwidth up to 0.3 and more.

II. Simplified Equivalent Representations

A. Exact Equivalent Circuit

Previously M. Onoda and the author reported the lumped-element equivalent representation for lossless multicoupled lines by using a half-angle Richards' variable ($\tilde{q}=2\tanh(j(\pi/4)(f/f_0))$, where f_0 is the quarter-wavelength frequency. In place of this $\tilde{q}$-variable, the following new variable q is considered:

$$q=2\tanh\left(j\frac{\pi}{4}\left(\frac{f}{f_0}-1\right)\right). \tag{1}$$

Richards' variable ($p=\tanh(j(\pi/4)(f/f_0))$ can be expressed by this q-variable as

$$p=(4+q^2)/4q. \tag{2}$$

Fig. 1 shows the frequency characteristics of this variable. In terms of this q-variable, the $2n$-port $ABCD$ matrix $[F]$ of the n-wire line of length l and characteristic impedance (or admittance) matrix $[Z_0]$ (or $[Y_0]$) is expressed by

Manuscript received November 1, 1979; revised April 1, 1980.

The author is with the Department of Electrical and Electronics Engineering, Tokyo Institute of Technology, Tokyo, Meguro-ku Ookayama 2-12-1, Japan 152.

0018-9480/80/0800-0852$00.75 ©1980 IEEE

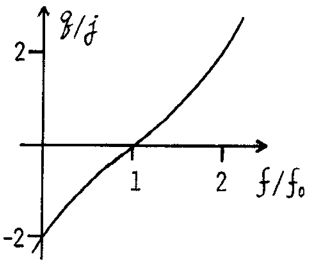

Fig. 1. The frequency characteristics of the q-variable.

the rational functions of q as

$$[F]=\frac{j}{4-q^2}\begin{bmatrix} 4q[1_n] & [Z_0](4+q^2) \\ [Y_0](4+q^2) & 4q[1_n] \end{bmatrix}. \quad (3)$$

Since this q-variable becomes zero at f_0, this frequency transformation leads to a BP to LP transformation. Equation (3) can be expressed in another form as

$$[F]=\frac{1}{\sqrt{1-(cq)^2}}\begin{bmatrix} [1_n] & aq[Z_0] \\ bq[Y_0] & [1_n] \end{bmatrix} \cdot \begin{bmatrix} 0 & j[Z_0] \\ j[Y_0] & 0 \end{bmatrix} \cdot \frac{1}{\sqrt{1-(cq)^2}}\begin{bmatrix} [1_n] & aq[Z_0] \\ bq[Y_0] & [1_n] \end{bmatrix} \quad (4a)$$

$$=\frac{j}{1-(cq)^2}\begin{bmatrix} (a+b)q[1_n] & (1+a^2q^2)[Z_0] \\ (1+b^2q^2)[Y_0] & (a+b)q[1_n] \end{bmatrix} \quad (4b)$$

where $a=b=c=1/2$.

The first term and the third term are $ABCD$ matrices of multiwire lines of length $l/2$ in the $(q/2)$-domain. The second term represents the ideal immittance–inverter bank. By cascade connecting circuits corresponding to each term of (4a), we can obtain the exact equivalent representation of the multicoupled lines in terms of the q-variable.

B. Simplified Equivalent Representations

In order to obtain simplified equivalent representations in the vicinity of $f=f_0$ $(q=0)$, we change the coefficients of q^2 terms in (3). These changes do not cause large error if we choose other values of a,b,c under the restriction of $a+b=1$ in (4b). The simplest representations are derived by choosing a) $a=1$, $b=c=0$, or b) $b=1$, $a=c=0$. Corresponding to these replacements, we obtain two types of simplified equivalent representations for multiwire lines by cascade connecting the circuits corresponding to each term of (4a) for both a) and b). The representations obtained for the case of $n=2$ are shown in Fig. 2(a) and (b). The two types of ideal immittance–inverter banks as shown in Fig. 2(a) and (b) are electrically equivalent.

Since the circuits in Fig. 2(a) and (b) are expressed by the values of characteristic impedance and admittance

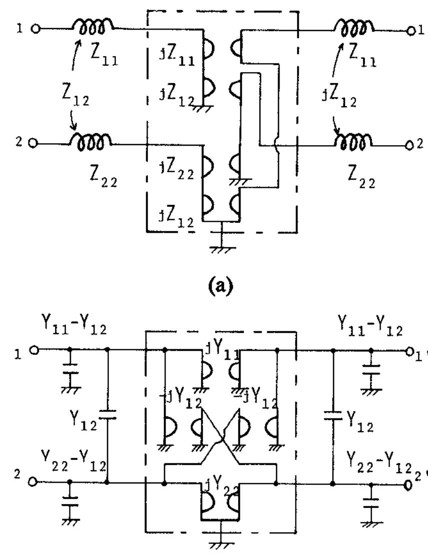

Fig. 2. Simplified equivalent circuits of multiwire lines ($n=2$). (a) Z-type representation. (b) Y-type representation.

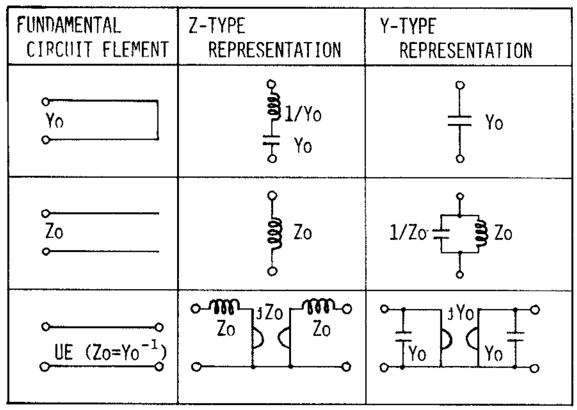

Fig. 3. Simplified equivalent circuits of fundamental circuit elements.

TABLE I
RELATIVE ERRORS OF OPEN-CIRCUITED LINE PERCENT

$(f/f_0)-1$	Z-type	Y-type
0.05	-0.154	0.466
0.10	-0.619	1.905
0.15	-1.400	4.452
0.20	-2.509	8.365
0.30	-5.760	22.47

matrices, respectively, we call them Z-type and Y-type representations, respectively. They are easily extended for the general cases of n-wire lines. Furthermore, fundamental circuit elements for commensurate-line-length networks can be expressed as shown in Fig. 3 by use of the derived two types of equivalent representations in the simple case of $n=1$.

The derived two types of representations were tested first theoretically with the line short- and open-circuited at the far end. Table I shows the relative errors of input impedances compared with the exact computations for the case of the line open-circuited at the far end. The relative error for the Z-type and Y-type representations is under 5 percent for $0.7 < f/f_0 < 1.3$ and $0.85 < f/f_0 < 1.15$, respectively.

In the case of the line short-circuited at the far end, the relative errors for each type of representation are the same as those in the case of the line open-circuited at the far end.

From these results it is concluded that two types of representations would be quite adequate for most narrow-band applications. In general, the Y-type representation is suitable for the analysis and the synthesis of circuits with comparatively many short-circuited terminals for reasons of easiness and accuracy. On the contrary, circuits with comparatively many open-circuited terminals can easily and accurately be analyzed and synthesized by the use of Z-type representation.

III. Design Method for Coupled-Line Filters

As an application of the derived equivalent representations, the general design method for coupled-line bandpass or bandstop filters is discussed. Design formulas for coupled-line bandpass or bandstop filters can be obtained by equating their equivalent circuits derived from the general equivalent representations of Fig. 2(a) and (b) to LC low-pass filters.

In designing these filters, one should first select the type of response function and the number of lines that yield the desired insertion loss function of ω in the pass and stopbands. If we denote the desired passband edges of coupled-line filters by f_1 and f_2, the quarter-wavelength frequency f_0 and the length of the lines l are determined as

$$f_0 = \frac{f_1 + f_2}{2} \qquad l = \lambda_0/4 \tag{5}$$

where λ_0 is the wavelength in transmission lines at f_0. Next the element values of the prototype filters may be computed and then the elements of the characteristic impedance $[Z_0]$ or admittance matrices $[Y_0]$ can be derived from the design formulas. This may be done with the aid of the following approximate relationship between the frequency scales of the prototype filters and the coupled-line filters

$$\Omega_c = 2\tan\left(\frac{\pi}{4}\,\frac{f_2 - f_1}{2f_0}\right) \tag{6}$$

where Ω_c is the cutoff frequency in the q-domain. Furthermore, the n-wire line dimensions should be determined to yield these matrices. These may be determined from various design charts [10].

In this paper, we show the procedure for deriving the design equations of a new bandpass filter as shown in Fig. 4. The design equations for well-known filters such as hairpin-line and interdigital-line filters are similarly derived. The advantages of filters of this new type are that they have fewer connections to ground than interdigital filters and they require fewer transmission lines than hairpin-line filters to realize the same order of bandpass filter.

The assumption of negligible capacitive couplings beyond the nearest neighbors (i.e., a sparse capacitance-matrix assumption) corresponds more closely to physical reality than the one neglecting inductive couplings beyond the nearest neighbors (i.e., a sparse inductance-matrix assumption) [6], [8]. However, the sparse capacitance-matrix assumption leads to very complex equivalent circuits for hairpin-line filters and filters of this type. By considering inductive couplings between not only nearest neighbors but next-nearest neighbors, the proposed design method leads to easier design procedure based to a first approximation on the assumption of a sparse $[Y_0]$ matrix.

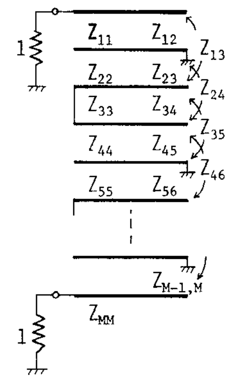

Fig. 4. A new bandpass filter.

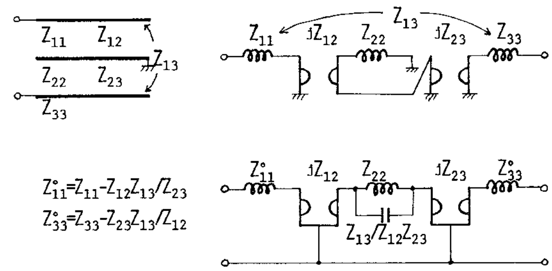

Fig. 5. Derivation of the equivalent circuit of the new bandpass filter.

First we derive the equivalent circuit of the section of Fig. 5(a). Boundary conditions are applied to the terminals of the Z-type representation of Fig. 2(a) with inductive couplings between next-nearest neighbors. Then open-circuited terminals disappear because they connect with series inductances and series inverters. We obtain an equivalent circuit as shown in Fig. 5(b). Reducing the mutual inductive couplings to a capacitance and inductances, we obtain the equivalent circuit shown in Fig. 5(c) of the section of Fig. 5(a). Because of a small influence to the narrow-band bandpass filter characteristics, we neglect the capacitance $(Z_{13}/Z_{12}Z_{23})$ in designing the filter. That leads to simpler design formulas.

For the general case where the inductive couplings between the nearest and next-nearest neighbors are considered, the equivalent circuit of the bandpass filter derived from the Z-type equivalent representation of Fig. 2(a) is shown in Fig. 6.

In Fig. 6, transformer sections are introduced as end sections to obtain realizable impedance levels in the interior of the filter. The circuits, which consist of inductances Z_{11}° (or Z_{MM}°) and a ideal inverter jZ_{11}° (or jZ_{MM}°), behave

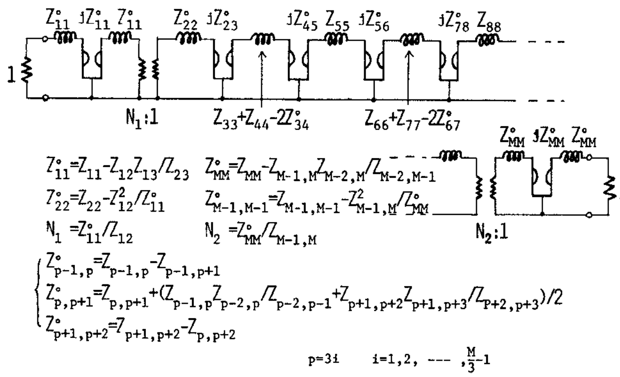

Fig. 6. Equivalent circuit of the new bandpass filter.

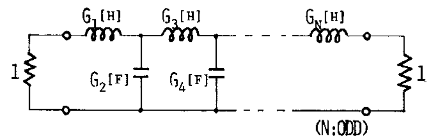

Fig. 7. Prototype LC low-pass filter.

TABLE II
DESIGN FORMULAS FOR THE NEW BANDPASS FILTER
($M=3(N+1)/2$)

$Z_{11}=2-1/(1+\Omega_c/G_1)$	$Z_{MM}=2-1/(1+\Omega_c/G_N)$	
$Z_{12}=\sqrt{h\Omega_c/G_1}$	$Z_{M-1,M}=\sqrt{h\Omega_c/G_N}$	
$Z_{22}=h(1+\Omega_c/G_1)$	$Z_{M-1,M-1}=h(1+\Omega_c/G_N)$	
$Z_{p+2,p+2}=h \quad (i\neq\frac{M}{3}-1)$ $Z_{p-1,p}=h\Omega_c/\sqrt{G_{2i-1}G_{2i}}(1-Cp)$ $Z_{p+1,p+2}=h\Omega_c/\sqrt{G_{2i}G_{2i+1}}(1-Cp)$		$p=3i$ $i=1,2,\cdots,\frac{M}{3}-1$
$Z_{pp}=Z_{p+1,p+1}=\frac{1}{2(1-Cp)}\left(h+\frac{Z_{p-1,p}^2}{Z_{p-1,p-1}}+\frac{Z_{p+1,p+2}^2}{Z_{p+2,p+2}}\right)$ $Z_{p,p+1}=CpZ_{pp}$		$p=3i$ $i=1,2,\cdots,\frac{M}{3}-1$
$Z_{j,j+2}=Z_{j,j+1}Z_{j+1,j+2}/Z_{j+1,j+1}$		$j=1,2,\cdots,M-2$
$[Y_0]=[Z_0]^{-1}$		

approximately like unit elements in the vicinity of the quarter-wavelength frequency (see Fig. 3). These characteristic impedances $Z_{11}^{\circ}, Z_{MM}^{\circ}$ are chosen equal to their terminations (1 Ω), so as not to alter the attenuation of the filter.

If $[Y_0]$ is assumed to be a sparse matrix, the relations between the element values of the $[Z_0]$ matrix which is the inverse matrix of $[Y_0]$ are given as

$$Z_{j,j+2}=Z_{j,j+1}Z_{j+1,j+2}/Z_{j+1,j+1}, \qquad j=1,2,\cdots,M-2. \tag{7}$$

By imposing the relations and by equating the prototype LC low-pass filter as shown in Fig. 7, whose cutoff frequency is normalized as 1, to the equivalent circuit of Fig. 6, we obtain the design formulas as shown in Table II, which are based to a first approximation on the assumption of a sparse $[Y_0]$ matrix.

The order N of the desired insertion-loss function must be an odd number and the number of transmission lines is given as $M=3(N+1)/2$.

In the design formulas, we use a coupling parameter C_p between the line pairs and an independent parameter h which controls impedance levels in the filter interiors. The coupling parameter C_p gives the relative degrees of "coupling" between line pairs. This is defined as

$$C_p=Z_{ij}/\sqrt{Z_{ii}Z_{jj}}, \qquad j=i+1 \tag{8}$$

where Z_{ij} are (i,j) element of the impedance matrix.

Generally all elements of the resulting $[Y_0]$ matrix have nonzero values, but all element values except those of the diagonals and the subdiagonals must be negligible because of (7). Then neglecting those element values, a sparse $[Y_0]$ matrix is obtained. The validity and accuracy of this design method is demonstrated by showing numerical examples in the next section.

IV. EXAMPLES OF DESIGN AND VERIFICATION OF DESIGN ACCURACY

The accuracy of both the equivalent representations and the design formulas were verified theoretically because of the approximations necessary in their derivation. This was done by exact computations of the insertion-loss responses of the actual coupled-line filter networks specified by the formulas for various bandwidths and for either maximally flat or equal-ripple responses. This paper shows the cases of the hairpin-line filter and of the new bandpass filter.

Figs. 8 and 9 show calculated insertion-loss responses for $N=5$ hairpin-line filters and $N=5$ bandpass filters of the new type, respectively. The theoretical responses computed using the exact network matrix are depicted by the solid lines in Figs. 8 and 9. Design data of bandpass filters of the new type are also shown in Table III.

The $[Y_0]$ matrix was first calculated using the design formulas of Table II. Table III shows the diagonal and subdiagonal values of the $[Y_0]$ matrix for the case of the new type of bandpass filters. And the other element values were under 10^{-2} and, therefore, negligible. Then the responses of all filters were computed based on a sparse capacitance-matrix assumption. They proved to be very accurate for relative bandwidths up to 0.3, and even at 0.4 the response is adequate for many applications.

In order to check the influence of inductive couplings beyond nearest neighbors, the responses were recalculated using the values derived by the same design procedures except neglecting the inductive couplings beyond nearest neighbors. The results are depicted by a dashed line in Fig. 9.

From the comparison, it is concluded that the proposed design method for bandpass filters of the new type gives exact designs based on a sparse capacitance matrix for any practical purposes up to 30-percent bandwidth and more.

If this design method is compared with design methods for half-wave parallel-coupled-line filters given by Cohn [4], hairpin-line filters given by Cristal and Frankel [6], [7], and an approximate design method by Matthaei [5], either method should give good results for filters of about 10 percent bandwidth or less. For bandwidth greater than

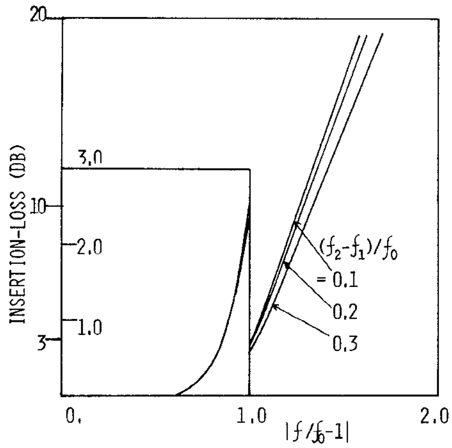

Fig. 8. Insertion-loss curves of hairpin-line filters designed for maximally flat responses ($N=5$, $h=1.5$, $C_p=0.1$).

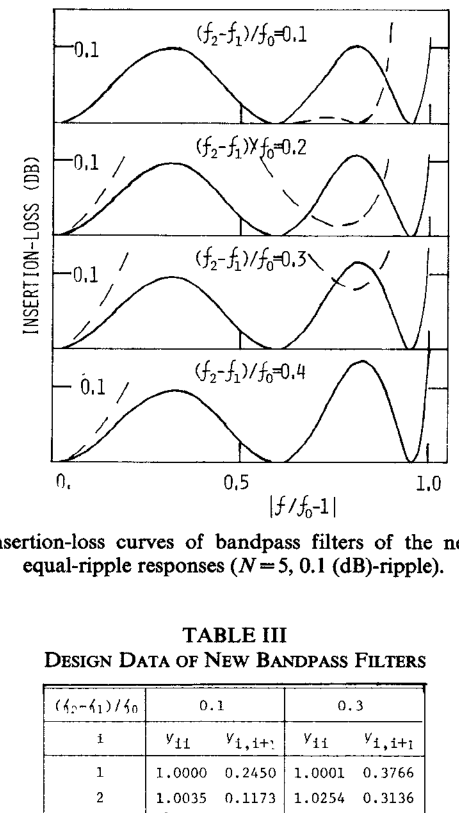

Fig. 9. Insertion-loss curves of bandpass filters of the new type for equal-ripple responses ($N=5$, 0.1 (dB)-ripple).

TABLE III
DESIGN DATA OF NEW BANDPASS FILTERS

$(f_2-f_1)/f_0$	0.1		0.3	
i	y_{ii}	$y_{i,i+1}$	y_{ii}	$y_{i,i+1}$
1	1.0000	0.2450	1.0001	0.3766
2	1.0035	0.1173	1.0254	0.3136
3	1.8195	0.1805	1.8237	0.1707
4	1.8140	0.0953	1.7890	0.2831
5	1.0101	0.0953	1.0906	0.2831
6	1.8140	0.1805	1.7890	0.1707
7	1.8195	0.1173	1.8237	0.3136
8	1.0035	0.2450	1.0254	0.3766
9	1.0000		1.0001	
Parameters	$h=1.0$ $Cp=0.1$			

about 10 or 15 percent, Cohn's method does not give accurate designs and the design equations described herein and those by Matthaei and Cristal are preferable. For bandwidth greater than about 30 or 40 percent, the proposed design technique does not give greater accuracy than that derived by Matthaei and Cristal.

However Matthaei's technique is confined to circuits which are exactly or approximately representable with unit elements and open- and short-circuited lines. It often requires special techniques to derive equivalent circuits of multiwire line networks expressed by unit elements and open- and short-circuited lines. Furthermore, the derivation of equivalent circuits based on the assumption of neglecting capacitive couplings beyond the nearest neighbors is more complicated in the case of hairpin-line filters and so forth. Even based on the assumption proposed herein as the first approximation of a sparse capacitance matrix, it is difficult to derive the equivalent circuits. The same things can be said about other approximate design methods.

While the new design method can lead to the equivalent circuits even more easily and does not require any special techniques, if we design the other types of bandpass or bandstop filters whose structures are more complicated, the new design method is preferable.

V. CONCLUSION

Simplified lumped-element equivalent representations for multiwire lines have been derived by introducing a new variable q. The derived two types of representations are equivalent for multiwire lines under 5-percent relative error in the frequency range $0.85 < f/f_0 < 1.15$. It is concluded that these equivalent representations are useful for both the analysis and the design of bandpass and bandstop commensurate-line length networks and coupled-line filters and directional couplers of narrow bandwidths, etc. As an application of the new representations, we derived a general design method, which can be applied to several types of coupled-line filters. Furthermore, the accuracies of the derived representations and design formulas were verified theoretically by using examples of hairpin-line filters and bandpass filters of the new type.

ACKNOWLEDGMENT

The author wishes to thank Prof. M. Onoda and Prof. T. Yanagisawa for advice and suggestions, and also wishes to thank the reviewers for their valuable comments on this paper.

REFERENCES

[1] R. Sato and E. G. Cristal, "Simplified analysis of coupled transmission-line networks," *IEEE Trans. Microwave Theory Tech.*, vol. MTT-18, pp. 122, 1970.

[2] M. Onoda and H. Kunieda, "Lumped-element equivalent representations of transmission-line network by half angle Richards' variable," in *IEEE 1978 Int. Symp. on CAS*, pp. 946, 1978.

[3] S. Kato and R. Sato, "A design method for coupled transmission line filters having an attenuation pole at origin," *Inst. Elect. Commun. Eng. Japan*, vol. 60-A, pp. 375, Apr. 1977 (in Japanese).

[4] S. B. Cohn, "Parallel-coupled transmission-line resonator filters," *IRE Trans. Microwave Theory Tech.*, vol. MTT-6, Apr. 1958.

[5] G. L. Matthaei, "Wide-band (and narrow-band) band-pass microwave filters on the insertion loss basis," *IRE Trans. Microwave Theory Tech.*, vol. MTT-8, Nov. 1960.

[6] E. G. Cristal and S. Frankel, "Hairpin-line and hybrid hairpin-line/half-wave parallel-coupled-line filters," *IEEE Trans. Microwave Theory Tech.*, vol. MTT-20, Nov. 1972.

[7] E. G. Cristal, "New design equations for a class of microwave

filters," *IEEE Trans. Microwave Theory Tech.*, vol. MTT-19, May 1971.
[8] U. H. Gysel, "New theory and design for hairpin-line filters," *IEEE Trans. Microwave Theory Tech.*, vol. MTT-22, May 1974.
[9] E. G. Cristal, "Microwave filters," in *Modern Filter Theory and Design* G. C. Temes and S. K. Mitra, Eds. New York: Wiley, 1973, pp. 273.
[10] T. A. Milligan, "Dimensions of microstrip coupled-lines and interdigital structures," *IEEE Trans. Microwave Theory Tech.*, vol. MTT-25, May 1977.

Propagation in a Rectangular Waveguide Periodically Loaded with Resonant Irises

MANUEL S. NAVARRO, MEMBER, IEEE, TULLIO E. ROZZI, SENIOR MEMBER, IEEE, AND YUEN TZE LO, FELLOW, IEEE

***Abstract*—In this contribution we treat the problem of an infinite rectangular waveguide periodically loaded by means of infinitely thin resonant irises.**

The method of solution breaks down the problem into two separate steps: 1) the multiport network characterization of the resonant iris; 2) the network analysis of the equivalent periodic network.

The results for the resonant iris can be used for various applications, such as the design of waveguide filters and matching networks. In the limiting cases of purely capacitive or inductive irises, the results agree exactly with existing experimental and numerical values.

The size of the eigenvalue equation to be solved for the periodic structure equals half the number of ports of the network characterization of the iris and is generally small (typically five to seven). The eigenvalues have good convergence properties with respect to the size of the matrix.

I. Introduction

In recent years the corrugated waveguide has found wide use in radar and communication systems. Significant research has been done on the problem of the circular corrugated waveguide. We distinguish three main approaches:

1) the modified boundary condition method, applicable only for a special value of the groove depth [1], [2];
2) the modified residue calculus technique [1], [3] applicable only for certain modal configurations;
3) mode matching technique [1] which is fairly general in applicability.

In the case of the rectangular guide, however, method 1) cannot be implemented analytically [3], [4]. Method 2) is altogether not applicable. Method 3) is also not applicable for this kind of geometry owing to the nonseparability of the configuration [4].

Brown in 1958 [5] suggested that a periodically loaded waveguide be modeled by means of a cascade of identical multiport reactances connected by a finite number of uncoupled transmission lines. Each reactance represents a discontinuity in the cascade, which causes coupling between waveguide modes otherwise uncoupled. Unfortunately, up to date this approach could not be actually implemented, due to the lack of proper multiport representation of the discontinuity.

Recently, however, a method for deriving lumped, wide-band equivalent networks of waveguide discontinuities has become available. The above has been applied to the problems of the inductive and capacitive iris and step [6], [7]. Apart from having inherently good convergence properties and involving manipulations with small matrices only, this approach separates the frequency and the geometry dependence, so that the analysis need not be repeated at each frequency point. A detailed discussion has been given elsewhere [6]–[8]. However, for the convenience of the reader, we recall here the concept of "accessible" and "localized" modes. Accessible modes are the waveguide modes that being excited at the location of one discontinuity, are "seen" by the adjacent discontinuities. This includes all the propagating modes of the original (unloaded) waveguide, plus, possibly, the first few evanescent ones, depending upon the separation between adjacent discontinuities.

Each accessible mode corresponds to a pair of accessible ports in the multimode equivalent network of the discontinuity. Between discontinuities, each accessible mode is described by means of a length of transmission line. All remaining modes, purely evanescent, are called localized, as they remain localized to the neighborhood of the discontinuity that excites them. The latter, collectively,

Manuscript received November 14, 1979; revised August 1, 1980.
M. S. Navarro was with the Department of Electrical Engineering, University of Illinois at Urbana, IL. He is now with the Deparmento de Electonica y Circuitos, Universidad Simon Bolivar, Caracas 108, Venezuela.
T. E. Rozzi is with the Department of Electrical Engineering and Electronics, University of Liverpool, Liverpool, L69 3BX U.K.
Y. T. Lo is with the Department of Electrical Engineering, University of Illinois, Urbana, IL.